International Journal of Modern Physics E
Vol. 28, No. 8 (2019) 1950066 (9 pages)

DOI: 10.1142/S0218301319500666

World Scientific
www.worldscientific.com

N-N-N^* model calculations for experimental η-mesic ^{3}He searches

N. G. Kelkar

Dept. de Fisica, Universidad de los Andes,
Cra.1E No.18A-10, Santafe de Bogotá, Colombia
nkelkar@uniandes.edu.co

H. Kamada

Department of Physics, Faculty of Engineering,
Kyushu Institute of Technology, Kitakyushu 804-8550, Japan
kamada@mns.kyutech.ac.jp

M. Skurzok

INFN, Laboratori Nazionali di Frascati,
Via E. Fermi, 40, 00044 Frascati (Roma), Italy

Institute of Physics, Jagiellonian University,
Prof. Stanisława Łojasiewicza 11,
30-348 Kraków, Poland
magdalena.skurzok@lnf.infn.it

Received 31 July 2019
Accepted 30 August 2019
Published 27 September 2019

The possibility for the existence of the exotic NNN^* states is explored with the objective of calculating the N^* momentum distribution inside such nuclei. Even though the latter is an essential ingredient for the analysis of the experimental data on the $pd \to pd\pi^0$, $pd \to ppp\pi^-$ and $pd \to pnn\pi^+$ reactions aimed at finding an η-mesic ^{3}He, the data analysis is usually performed by approximating the N^* momentum distribution by that of a nucleon. Here, we present calculations performed by solving the three-body Faddeev equations to obtain the momentum distribution of the N^* inside possible $(N^*)^+np$, $(N^*)^0np$ and $(N^*)^+$-d states. The N^* momentum distributions are found to be much narrower than those of the nucleons and influence the data selection criteria.

Keywords: Searches of η-mesic nuclei; exotic quasibound states; N^* resonance.

PACS Number(s): 21.85.+d, 21.45.−v, 14.20.Gk

1. Search for Exotic States

The past few decades have seen extensive searches of various exotic states of mesons and nuclei.[1] Unstable bound states of the neutral η mesons and nuclei is one such example which has been hard to find experimentally (see Refs. 2–5 for reviews on

the experimental as well as theoretical searches). Though a clear and conclusive evidence for the existence of η-mesic nuclei has still not been found (see, however, Ref. 6 and the claim in Ref. 7 which was re-examined in Ref. 8 where the authors attributed the peak structure to an artifact arising from the complicated background structure of quasi-free pion production) there are several indications of its existence. For example, η production with protons scattered on light nuclei such as the deuteron[9] and with photons on ^{3}He[8,10] show sharply rising amplitudes at energies close to threshold. This is usually taken as an indication of the strong η-nucleus interaction which could make the existence of an η-mesic nucleus possible.

An important ingredient in the search for η-mesic nuclei is the S11 $N^*(1535)$ resonance. Experimental analyses for the formation of an η-mesic nucleus[11–13] assume the η-nucleon interaction to proceed via the formation of an N^* resonance as an intermediate state. For example, the analysis in Ref. 12 for the search of an η-mesic ^{4}He is carried out by assuming the reaction to proceed as $dd \rightarrow (^4\text{He}\text{-}\eta)_{\text{bound}} \rightarrow (N^*\text{-}^3\text{He}) \rightarrow {}^3\text{He}\, N\pi$. Therefore, for such a reaction below the η meson production threshold, an off-shell η meson produced in a dd collision, is assumed to be absorbed on one of the nucleons in the helium nucleus and may propagate inside the nucleus by consecutive excitations and decays of the N^* to a nucleon and η (off-shell) until it finally decays into an on-shell pion and a nucleon. Thus, in principle, within this description, as long as the η-mesic state exists, an N^* also exists inside the nucleus. It is then natural to ask if one can consider the existence of unstable bound states of N^* and nuclei.[14] If they do exist, one can investigate the motion of a bound N^* inside the nucleus. Such an investigation was carried out in Refs. 14 and 15 and loosely bound N^*-nuclear states with a large decay width were found in case of N^*-^{3}He and N^*-^{24}Mg.

In this work, we investigate the possibility for N^*NN bound states to exist and if they do, calculate the momentum distribution of the N^* inside such exotic nuclei. The motivation for such an undertaking comes from the fact that the N^* momentum distribution is an important input for simulations done by the experimentalists in order to determine the kinematics and detector acceptance in the analysis of data on the $pd \rightarrow pd\pi^0$, $pd \rightarrow ppp\pi^-$ and $pd \rightarrow pnn\pi^+$ reactions aimed at finding an η-mesic ^{3}He nucleus.[16] In the absence of a calculation such as the present one, the data analysis is carried out by approximating the N^* momentum distribution by that of a nucleon inside ^{3}He. The results of the three-body Faddeev calculations of this work show that the above assumption is not appropriate and provides the necessary distributions for a better experimental analysis.

2. Three-Body Calculations for the Motion of N^* in N^*NN States

Three-body bound state calculations are often performed by solving Faddeev equations in a partial wave basis. In Ref. 18, however, a new way of solving the Faddeev

equations directly as a three-dimensional (3D) integral equation without employing partial wave decomposition was proposed. The method has since then been applied for the study of different systems. This kind of a nonpartial-wave approach has been applied for the investigation of exotic states like the $\alpha\Lambda\Lambda$[19] as well as atomic systems[20] such as the ^{4}He dimer. In this work, we shall follow the approach proposed in Ref. 18 and solve the Faddeev equations to find bound states of the N^* and two nucleons. For details of the three-body formalism, we refer the reader to Ref. 18 and explain the theoretical framework only briefly.

2.1. *Elementary potentials*

The N^*–n and N^*–p interaction is written using the one-pion and η exchange potential with the same diagrams and assumptions as in Ref. 15. In principle, there could be additional contributions from two pion exchange (ρ meson exchange diagram) and other box diagrams. However, considering the exploratory nature of this work and also the fact that there is no data available to fix the $NN^* \to NN^*$ potentials, we leave such an undertaking for the future.

To remind the reader briefly, in Fig. 1, we show the diagrams considered for example for the propagation of a positive N^*. Diagrams involving the $N^*N^*\pi$ or $N^*N^*\eta$ couplings which are hardly known will not be considered. Apart from the couplings being unknown, the potential in this case turns out to be spin dependent (and so also suppressed as compared to the leading term in the potential of Fig. 1). The πNN^* and ηNN^* couplings (with $N^*(1535,1/2^-)$) are given by the following interaction Hamiltonians[21]:

$$\begin{aligned} \delta H_{\pi NN^*} &= g_{\pi NN^*}\bar{\Psi}_{N^*}\boldsymbol{\tau}\Psi_N \cdot \boldsymbol{\Phi}_\pi + \text{h.c.} \\ \delta H_{\eta NN^*} &= g_{\eta NN^*}\bar{\Psi}_{N^*}\Psi_N \cdot \Phi_\eta + \text{h.c.} \end{aligned} \tag{1}$$

Using the standard Feynman diagram rules and including an off-shellness at the vertices through form factors containing the parameters Λ_π and Λ_η (see Ref. 15 for details), the momentum space forms of the elementary potentials used in this work

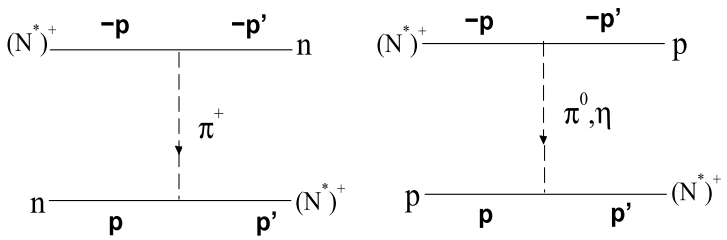

Fig. 1. Elementary $NN^* \to NN^*$ processes considered in this work.

are given by

$$V_{(N^*)^+p}(|\mathbf{p}-\mathbf{p}'|) = -\frac{g^2_{N^*\pi}}{|\mathbf{p}-\mathbf{p}'|^2+m_\pi^2}\left(\frac{\Lambda_\pi^2-m_\pi^2}{\Lambda_\pi^2+|\mathbf{p}-\mathbf{p}'|^2}\right)^2 - \frac{g^2_{N^*\eta}}{|\mathbf{p}-\mathbf{p}'|^2+m_\eta^2}\left(\frac{\Lambda_\eta^2-m_\eta^2}{\Lambda_\eta^2+|\mathbf{p}-\mathbf{p}'|^2}\right)^2, \quad (2)$$

$$V_{(N^*)^+n}(|\mathbf{p}-\mathbf{p}'|) = -\frac{g^2_{N^*\pi}}{|\mathbf{p}-\mathbf{p}'|^2+m_\pi^2}\left(\frac{\Lambda_\pi^2-m_\pi^2}{\Lambda_\pi^2+|\mathbf{p}-\mathbf{p}'|^2}\right)^2 (\tau_1\cdot\boldsymbol{\tau}_2),$$

where g_{N^*x} (with $x=\pi$ and η) are the coupling constants at the $N^*N\pi$ and $N^*N\eta$ vertices and are chosen from the available values given in literature (see Table 1 of Ref. 15). The factor in big round brackets takes care of the off-shell nature of the exchanged mesons. The elementary potentials for the $(N^*)^0$ interaction with a nucleon can be written in a similar way. The isospin operator $(\boldsymbol{\tau}_1\cdot\boldsymbol{\tau}_2)$ gives a factor of 2 in this case. The choice of the neutron–proton potential entering the calculation of $(N^*)^+-n-p$ three body bound state calculation is that of a Malfliet–Tjon type potential given by a Yukawa overlap form as in[22]:

$$V_{np}(|\mathbf{p}-\mathbf{p}'|) = -\frac{V_a}{2\pi^2}\frac{1}{\mu_a^2+|\mathbf{p}-\mathbf{p}'|^2}+\frac{V_r}{2\pi^2}\frac{1}{\mu_r^2+|\mathbf{p}-\mathbf{p}'|^2}, \quad (3)$$

with $V_a = 3.1769\,\mathrm{fm}^{-1}$, $\mu_a = 305.86\,\mathrm{MeV}$, $V_r = 7.291\,\mathrm{fm}^{-1}$ and $\mu_r = 613.69\,\mathrm{MeV}$. In case of the $(N^*)^0-p-p$ system, we also consider a Yukawa overlap form which is linked to the $^1\mathrm{S}_0$ partial wave of the Reid Soft Core potential.[23]

2.2. *Faddeev equations and momentum distributions*

As mentioned above, we directly solve the three-body Faddeev equations by the method without partial wave decomposition.[18] The realistic nucleon–nucleon potential like a meson theoretical version includes the operators of the spin-orbit and the tensor force. The method is extended to apply on such operator-form potential.[24] Since our potentials in Eqs. (2) and (3) are only of a scalar form except for the isospin part, therefore, the simple method of Ref. 18 is enough to solve our Faddeev equations.

Here, we would briefly like to introduce the equations and the method. The degrees of freedom by selecting coordinates fixed to the nucleus can be reduced only to 3 because of the body-fixed frame. Taking the center-of-mass system, we use two Jacobi momenta $\mathbf{p}$ and $\mathbf{q}$. Figure 2 shows three sets of the momenta for each particle channel. For instance, the subscript i of the momenta corresponds to the spectator label of the ith particle. The three variables of the wave function are given by the magnitudes of the Jacobi momenta p_i, q_i and the angle θ_i between the

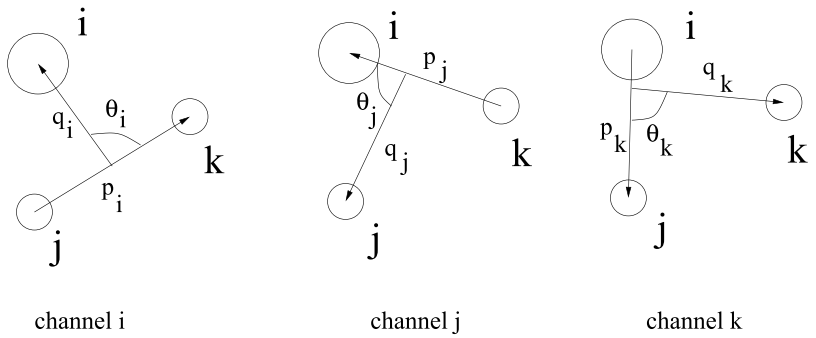

Fig. 2. Jacobi coordinates (**p**, **q**) of the three-body system. The subscript i in the coordinates signifies the ith spectator particle.

momenta.

$$\mathbf{p}_i \equiv \frac{m_j \mathbf{k}_k - m_k \mathbf{k}_j}{m_j + m_k}, \tag{4}$$

$$\mathbf{q}_i \equiv \frac{(m_j + m_k)\mathbf{k}_i - m_i(\mathbf{k}_j + \mathbf{k}_k)}{m_i + m_j + m_k}, \tag{5}$$

$$\cos\theta_i \equiv \frac{\mathbf{p}_i \cdot \mathbf{q}_i}{p_i q_i}, \tag{6}$$

The other momenta $\mathbf{p}_j$, $\mathbf{q}_j$, $\mathbf{p}_k$ and $\mathbf{q}_k$ are given by the ith momenta $\mathbf{p}_i$ and $\mathbf{q}_i$.

$$\mathbf{p}_j = -\frac{m_i}{m_k + m_i}\mathbf{p}_i - \frac{m_k(m_1 + m_2 + m_3)}{(m_k + m_i)(m_j + m_k)}\mathbf{q}_i, \tag{7}$$

$$\mathbf{p}_k = -\frac{m_i}{m_i + m_j}\mathbf{p}_i + \frac{m_j(m_1 + m_2 + m_3)}{(m_j + m_k)(m_i + m_j)}\mathbf{q}_i, \tag{8}$$

$$\mathbf{q}_j = \mathbf{p}_i - \frac{m_j}{m_j + m_k}\mathbf{q}_i, \tag{9}$$

$$\mathbf{q}_k = -\mathbf{p}_i - \frac{m_k}{m_j + m_k}\mathbf{q}_i, \tag{10}$$

where $\mathbf{k}_i$ is the intrinsic particle momentum and m_i is the ith particle mass. The wave function Ψ consists of the Faddeev components ψ_i ($i = 1, 2,$ and 3);

$$\Psi = \psi_1 + \psi_2 + \psi_3.$$

The components satisfy the Faddeev equations

$$\psi_i(\mathbf{p}_i, \mathbf{q}_i) = \langle \mathbf{p}_i \mathbf{q}_i \,|\, \psi_i \rangle = \psi_i(p_i, q_i, \theta_i) \tag{11}$$

$$= G_0 \int d^3 p_i' t_i(\mathbf{p}_i, \mathbf{p}_i') \langle \mathbf{p}_j' \mathbf{q}_j' \,|\, \psi_j \rangle + G_0 \int d^3 p_i'' t_i(\mathbf{p}_i, \mathbf{p}_i'') \langle \mathbf{p}_k'' \mathbf{q}_k'' \,|\, \psi_k \rangle, \tag{12}$$

where $\mathbf{p}_j$ and $\mathbf{q}'_j$ are functions of $\mathbf{p}'_i$ and $\mathbf{q}_i$, and, $\mathbf{p}''_k$ and $\mathbf{q}''_k$ are also functions of $\mathbf{p}''_i$ and $\mathbf{q}_i$, respectively, and t_i and G_0 are the two-body t-matrix and the three-body free Green's function, respectively.

Equation (12) is regarded as an eigen value equation. The binding energy is found when the eigen value equals to 1. Arnold's method for the equation is used in Ref. 18.

Performing calculations for two parameter sets, $g_{N^*\pi} = 1.09$, $g_{N^*\eta} = 2.07$ (which we shall refer to as Set 1)[25] and $g_{N^*\pi} = 1.05$, $g_{N^*\eta} = 1.6$ (Set 2)[26] we find the $(N^*)^+ - n - p$ system to be bound by $E_b = -2.75\,\text{MeV}$ in case of Set 1 but not bound with Set 2. The $(N^*)^0 - p - p$ system is not bound in any case. The parameter $\Lambda_\pi = 1.3\,\text{GeV}$ and $\Lambda_\eta = 1.5\,\text{GeV}$ in both cases. The relative momentum distribution of the N^* and the two nucleons inside the three body bound states can be evaluated as

$$T(q) = \frac{1}{4\pi} \int \Psi(\mathbf{p}, \mathbf{q})^2 d\mathbf{p} q^2 d\Omega_q, \tag{13}$$

where $\mathbf{q}$ is the $(N^*)^+ - (np)$ relative momentum and $\mathbf{p}$, the two-nucleon momentum vector. $T(q)$ is normalized such that

$$4\pi \int_0^\infty T(q) dq = 1. \tag{14}$$

In Fig. 3, the momentum distributions corresponding to the above $(N^*)^+ - n - p$ state and the $(N^*)^+$-deuteron state are shown. Considering the deuteron binding energy of 2.22 MeV and subtracting it from $E_b = -2.75\,\text{MeV}$ of the 3-body bound state, $(N^*)^+ - n - p$, the N^*-deuteron separation energy is $-0.53\,\text{MeV}$. The

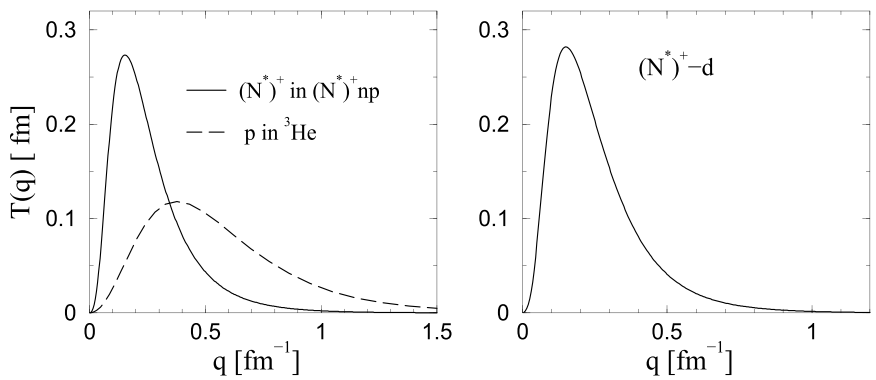

Fig. 3. (a) Momentum distribution of a positive N^* inside a three-body bound $(N^*)^+ - n - p$ (with a binding energy of $-2.75\,\text{MeV}$) as compared to that of a proton inside ^{3}He[27] and (b) the relative momentum distribution of a positive N^* and a deuteron inside a bound N^*-(np) state with (np) being a deuteron (normalized to 1).

momentum distribution in this case is calculated as

$$T(q)_{N^*d} = \frac{1}{4\pi}\int\left(\int \Psi(\mathbf{p},\mathbf{q})\phi_d(\mathbf{p})d\mathbf{p}\right)^2 q^2 d\Omega_q, \tag{15}$$

where $\mathbf{q}$ and $\mathbf{p}$ are the N^*-d and $n-p$ relative momenta. The normalization of $T(q)$, namely,

$$N_d = 4\pi\int T(q)_{N^*d}dq, \tag{16}$$

gives the probability to find a bound deuteron inside the three-body $(N^*)^+ - n - p$ bound state and is found to be 0.7163. The momentum distribution shown in Fig. 3 (solid line [b]) corresponds to the calculated $T(q)$ divided by 0.7163 (and is hence normalized to 1).

In order to note the difference between the nucleon and N^* momentum distributions inside the N^*NN states, in Fig. 4, we compare these momentum distributions inside the $(N^*)^+np$ and $(N^*)^0np$ states. It is interesting to note that the neutron distributions are quite similar in both systems. However, the existence of the Coulomb force between the $(N^*)^+$ and the proton causes the proton distribution in $(N^*)^+np$ to slightly increase in the smaller momentum region as compared to that in $(N^*)^0np$.

A few remarks about the implication of the existence of the exotic N^*NN states in the context of the experimental η-mesic search are in order here. Considering the model where the N^* propagates inside the nucleus and eventually decays by $N^* \to \pi N$, we have the following possibilities for the decay of the N^*NN states: (i) $(N^*)^+np \to \pi^+nnp$, (ii) $(N^*)^+np \to \pi^0pnp$, (iii) $(N^*)^0pp \to \pi^0npp$ and (iv) $(N^*)^0pp \to \pi^-ppp$. The WASA data which is being analyzed involves all possible

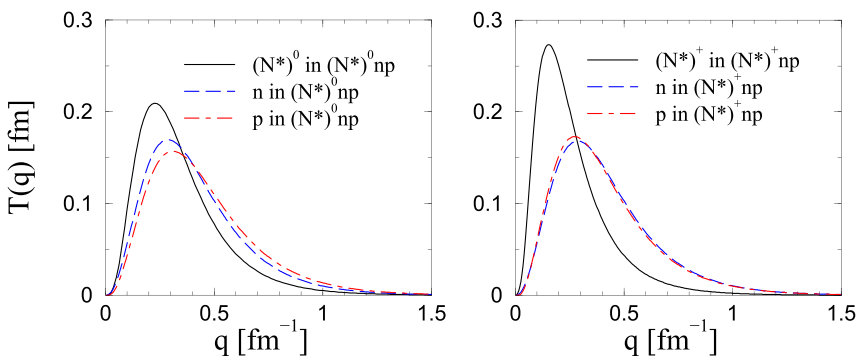

Fig. 4. (a) Comparison of the momentum distributions of an N^* (solid line), proton (dot-dashed line) and neutron (dashed line) inside the bound $(N^*)^0 - n - p$ (left panel) and $(N^*)^+ - n - p$ (right panel) states.

channels of the reaction, $pd \to NNN\pi$, with $N = p$ or n. The nonexistence of an $(N^*)^0pp$ state (within the model of the present work) would imply that it is not likely to observe the η-mesic ^{3}He state in the channel, $pd \to ppp\pi^-$. The existence of the $(N^*)^+np$ state implies that the likely channels to find η-mesic ^{3}He are, $pd \to nnp\pi^+$ and $pd \to npp\pi^0$. We note that since the binding energy of these exotic states is small, the Coulomb interaction also plays a role in deciding if the system is bound or not. The $(N^*)^0pp$ system is not bound but the $(N^*)^0np$ is found to be bound. If we would neglect the Coulomb force between the two protons, the $(N^*)^0pp$ would also be bound by about 0.8 MeV.

We remind the reader that in our calculations, the NN force of the N^*pp (N^*nn) system is taken to be the Reid Soft Core potential which is used only in the $^1S_0$ state. The $^1S_0$ state has no bound state. For the NN force of the N^*np system, we take the Malfliet–Tjon potential which takes into account both the $^1S_0$ and $^3S_1$ states. Therefore, the Malfliet–Tjon potential has a deuteron bound state. Taking the isospin breaking into account in this manner, we cannot expect the $(N^*)^0pp$ and $(N^*)^+np$ to be equally bound.

Finally, in order to note the implications of the N^* momentum distribution being narrower than that of the nucleon, simulations are performed in a similar manner as in Ref. 12 but for the pd reactions. In case of the $(^3\text{He-}\eta)_{\text{bound}}$ production in proton–deuteron collision, simulations of the $pd \to (^3\text{He-}\eta)_{\text{bound}} \to N^* - d \to dp\pi^0$ reaction performed with the N^* momentum distributions presented in Fig. 3 result in a significantly lower geometrical acceptance of the simultaneous registration of all outgoing particles in the WASA detector in comparison to those using the proton momentum distribution inside ^{3}He. To be specific, the acceptance is 0.267 and 0.261 for the $(N^*)^+$ in $(N^*)^+ - n - p$ and $(N^*)^+ - d$, respectively as compared to 0.635 found using the momentum distribution of a proton in ^{3}He.[27]

3. Summary

The possibility for the existence of the N^*NN bound states is explored with the objective of calculating the momentum distribution of the N^* inside such nuclei. The motivation for this work comes from the need for such a distribution in the analysis of the experimental data searching for η-mesic ^{3}He nuclei. The data on the $pd \to pd\pi^0$, $pd \to ppp\pi^-$ and $pd \to pnn\pi^+$ reactions is analyzed within a model which assumes the formation, propagation and decay of an N^* resonance as an intermediate step. For example, if an η-mesic ^{3}He is formed, the reaction $pd \to pd\pi^0$ is considered to proceed as $pd \to (\eta\text{-}^3\text{He})_{\text{bound}} \to (N^*)^+ - d \to pd\pi^0$. A knowledge of the motion of the N^* is necessary for simulations performed to calculate the kinematics and the geometrical acceptance of the detectors. The analysis of data[28] is usually carried out by approximating the momentum distribution of an N^* by that of a nucleon inside the nucleus. This work aims at improving this situation by providing the N^* distributions for data analysis.

Acknowledgments

The authors are thankful to Prof. P. Moskal for many useful discussions. One of the authors (N.G.K.) thanks the Faculty of Science, Universidad de los Andes, Colombia for financial support through Grant No. P18.160322.001-17. H. K. is thankful to the Japan Society for the Promotion of Science (JSPS) for financial support by Grant-in-Aid for Scientific Research (B) No. 16H04377. The numerical calculations were partially performed on the interactive server at RCNP, Osaka University, Japan.

References

1. S. Wycech, *Acta Phys. Pol. B* **41** (2010) 2201.
2. Q. Haider and L. C. Liu, *Int. J. Mod. Phys. E* **24** (2015) 1530009.
3. H. Machner, *J. Phys. G* **42** (2015) 043001.
4. B. Krusche and C. Wilkin, *Prog. Part. Nucl. Phys.* **80** (2014) 43.
5. N. G. Kelkar, K. P. Khemchandani, N. J. Upadhyay and B. K. Jain, *Rep. Prog. Phys.* **76** (2013) 066301.
6. G. A. Sokol and L. N. Pavlyuchenko, *Phys. Atom. Nucl.* **71** (2008) 509.
7. M. Pfeiffer *et al.*, *Phys. Rev. Lett.* **92** (2004) 252001.
8. F. Pheron *et al.*, *Phys. Lett. B* **709** (2012) 21.
9. J. Smyrski *et al.*, *Phys. Lett. B* **649** (2007) 258.
10. T. Mersman *et al.*, *Phys. Rev. Lett.* **98** (2007) 242301.
11. W. Krzemien, P. Moskal and M. Skurzok, *Acta Phys. Polon. B* **46** (2015) 757; M. Skurzok, W. Krzemien, O. Rundel and P. Moskal, *EPJ Web Conf.* **117** (2016) 02005; P. Adlarson *et al.*, *Phys. Rev. C* **87** (2013) 035204.
12. P. Adlarson *et al.*, *Nucl. Phys. A* **959** (2017) 102.
13. M. Skurzok *et al.*, *Phys. Lett. B* **782** (2018) 6.
14. N. G. Kelkar, D. Bedoya Fierro and P. Moskal, *Acta Phys. Pol. B* **47** (2016) 299.
15. N. G. Kelkar, *Eur. Phys. J A* **52** (2016) 309.
16. O. Rundel *et al.*, *Acta Phys. Pol. B* **48** (2017) 1807.
17. M. Skurzok *et al.*, *EPJ Web Conf.* **181** (2018) 01014; arXiv:1712.06307.
18. Ch. Elster *et al.*, *Few-Body Syst.* **27** (1999) 83.
19. H. Kamada *et al.*, *JPS Conf. Proc.* **17** (2017) 033012.
20. M. R. Hadizadeh and L. Tomio, *Few-Body Syst.* **54** (2013) 2227.
21. B. Lopez Alvaredo and E. Oset, *Phys. Lett. B* **324** (1994) 125.
22. Ch. Elster, J. H. Thomas and W. Glöckle, *Few-Body Syst.* **24** (1998) 55.
23. R. V. Reid, Jr., *Ann. Phys.* **50** (1968) 411.
24. J. Golak *et al.*, *Few-Body Syst.* **54** (2013) 2427.
25. C. S. An and B. Saghai, *Phys. Rev. C* **84** (2011) 045204.
26. E. J. Garzon and E. Oset, *Phys. Rev. C* **91** (2015) 025201.
27. A. Nogga, Nuclear and hypernuclear 3 and 4 body bound states, Ph.D. thesis, Ruhr Universität, Bochum (2001), available at http://www-brs.ub.ruhr-uni-bochum.de/netahtml/HSS/Diss/NoggaAndreas/.
28. O. Rundel, *EPJ Web Conf.* **199** (2019) 02029.